

MOL #47985

## **Hydrogen sulfide inhibits rotenone-induced apoptosis via preservation of mitochondrial function**

Li-Fang Hu, Ming Lu, Zhi-Yuan Wu, Peter T.-H. Wong, Jin-Song Bian\*

Department of Pharmacology, Yong Loo Lin School of Medicine, National University of  
Singapore, Singapore

MOL #47985

**Running title:** H<sub>2</sub>S inhibits rotenone-induced cell apoptosis

**Address corresponding to:**

Dr. Jin-Song Bian, MD, PhD

Assistant Professor,

Department of Pharmacology, Yong Loo Lin School of Medicine, National University of  
Singapore, Singapore, 117597

Email: [phcbjs@nus.edu.sg](mailto:phcbjs@nus.edu.sg).

Phone: (65)-6516-5502 Fax: (65)-6873-7690

Number of text pages: 26

Number of tables: 0

Number of figures: 10

Number of references: 32

Number of words in abstract: 183

Number of words in introduction: 506

Number of words in discussion: 1023

**Abbreviations:** CBS, cystathionine  $\beta$ -synthase; CSE, cystathionine  $\gamma$ -lyase; CNS, central nervous system; H<sub>2</sub>S, Hydrogen sulfide; 5-HD, 5-hydroxydecanoate; mitoK<sub>ATP</sub> channel, mitochondrial ATP-sensitive potassium channel; MAPK, mitogen-activated protein kinase;  $\Delta\Psi_m$ , mitochondrial membrane potential; NaHS, sodium hydrosulfide; PD, Parkinson's disease; PARP, Poly (ADP-ribose) polymerase

MOL #47985

## Abstract

Hydrogen sulfide (H<sub>2</sub>S) has been proposed as a novel neuromodulator, which plays critical roles in the central nervous system (CNS) affecting both neurons and glial cells. However, its relationship with neurodegenerative diseases is unexplored. The present study was undertaken to investigate the effects of H<sub>2</sub>S on cell injury induced by rotenone, a commonly used toxin in establishing *in vivo* and *in vitro* Parkinson's disease (PD) models, in human-derived dopaminergic neuroblastoma cell line (SH-SY5Y). We report here that sodium hydrosulfide (NaHS), an H<sub>2</sub>S donor, concentration-dependently suppressed rotenone-induced cellular injury and apoptotic cell death. NaHS also prevented rotenone-induced p38- and JNK- MAPK phosphorylation and rotenone-mediated changes in Bcl-2/Bax levels, mitochondrial membrane potential ( $\Delta\Psi_m$ ) dissipation, cytochrome *c* release, caspase-9/3 activation and poly (ADP-ribose) polymerase (PARP) cleavage. Furthermore, 5-hydroxydecanoate (5-HD), a selective blocker of mitochondrial ATP-sensitive potassium (mitoK<sub>ATP</sub>) channel, attenuated the protective effects of NaHS against rotenone-induced cell apoptosis. Thus, we demonstrated for the first time that H<sub>2</sub>S inhibited rotenone-induced cell apoptosis via regulation of mitoK<sub>ATP</sub> channel/ p38- & JNK-MAPK pathway. Our data suggest that H<sub>2</sub>S may have potential therapeutic value for neurodegenerative diseases, such as PD.

MOL #47985

## Introduction

Although it has been the conventional view that hydrogen sulfide (H<sub>2</sub>S) is a noxious gas, there is now accumulating evidence that it is an endogenously produced gaseous messenger and in particular, serves as an important neuromodulator in central nervous system (CNS) (Abe and Kimura, 1996; Kimura, 2002). The production of H<sub>2</sub>S in mammalian systems has been attributed to two pyridoxal-5'-phosphate-dependent enzymes: cystathionine β-synthase (CBS) and cystathionine γ-lyase (CSE), both of which use L-cysteine as a substrate (Qu et al., 2008). In human, rat and bovine brain, CBS, which is highly expressed in hippocampus and cerebellum, has been identified to be the main enzyme responsible for the biosynthesis of H<sub>2</sub>S (Abe and Kimura, 1996). The endogenous level of H<sub>2</sub>S in the brain has been reported to be in micromolar concentration range, much higher than that of plasma levels. The cytoprotective and cytotoxic effects of H<sub>2</sub>S in various model systems were summarized and reviewed by Szabo (Szabo, 2007).

Physiologically, H<sub>2</sub>S regulates N-methyl-D-aspartate (NMDA) receptor-mediated response and thus facilitates the induction of long-term potentiation (LTP) (Eto et al., 2002b; Kimura, 2000). H<sub>2</sub>S also induces calcium waves/elevation in both astrocytes and microglia (Lee et al., 2006; Nagai et al., 2004). Pathophysiologically, disturbed H<sub>2</sub>S synthesis in the brain has been reported in patients with Alzheimer's disease, Down's syndrome, and stroke (Eto et al., 2002a; Qu et al., 2006). We recently found that H<sub>2</sub>S attenuates lipopolysaccharide (LPS)-induced inflammation by inhibiting p38 mitogen-activated protein kinase (MAPK) in microglia (Hu et al., 2007). Kimura and his colleagues have demonstrated that H<sub>2</sub>S enhances neuronal activities and protects neurons against oxidative stress via increasing intracellular glutathione levels (Kimura and

MOL #47985

Kimura, 2004; Umemura and Kimura, 2007). The major intracellular targets of H<sub>2</sub>S described in the literature include ATP-sensitive potassium (K<sub>ATP</sub>) channels and a growing list of intracellular signaling molecules, notably, NF-κB and p38 MAPK. Among these, the action of H<sub>2</sub>S on K<sub>ATP</sub> channels received more attention (Wang, 2002; Yang et al., 2005). We recently reported H<sub>2</sub>S decreases blood pressure in freely moving rats via opening K<sub>ATP</sub> channels in hypothalamus (Dawe et al., 2008). Thus, H<sub>2</sub>S may play important roles in regulating CNS functions. Abnormal H<sub>2</sub>S production may contribute to the pathogenesis of different brain diseases.

Parkinson's disease (PD) is a neurodegenerative disorder characterized by symptoms including rigidity, resting tremor and instability of gait and posture. Increasing scientific evidence has demonstrated that microglia-mediated neuroinflammation is critical for the initiation and development of neurodegenerative disorders such as PD. Chemical compounds possessing anti-neuroinflammatory properties are being considered as promising candidates for PD therapy. Rotenone, which is widely used as a pesticide, has been shown to induce degeneration of dopaminergic neurons in animal models leading to behavioral and pathological symptoms similar to those of PD (Fleming et al., 2004). To follow up our previous observation that H<sub>2</sub>S produces anti-neuroinflammatory effects in microglia (Hu et al., 2007), we investigated the effects of H<sub>2</sub>S on cell apoptosis/injury in rotenone-treated human-derived dopaminergic neuroblastoma (SH-SY5Y) cells to evaluate if H<sub>2</sub>S may be of potential therapeutic value in the treatment of neurodegenerative diseases, such as PD.

## Materials and methods

MOL #47985

Reagents and antibodies. SB203580 and SP600125 were from Calbiochem (California, USA). All other chemicals used in this study were purchased from Sigma (Sigma, St. Louis, MO). Antibodies against phospho-JNK (Thr183 and Tyr185), caspase-3, phospho- and total-ERK1/2, Bax and Bcl-2 were purchased from Cell Signaling (Beverly, MA, USA). Antibodies for detecting cytochrome *c*, total- and phospho-p38 (Thr 180 and Tyr182) and total JNK1 were obtained from Santa Cruz (Santa Cruz Biotechnology Inc., CA, USA).

Rotenone solution in dimethyl sulfoxide (DMSO) was freshly prepared prior to each treatment. Final DMSO concentration in media did not exceed 0.05%. Because rotenone is lipophilic and may bind to proteins present in the serum, cells were transferred into lower serum media (0.5% fetal bovine serum, FBS) before rotenone treatment to prevent excessive retention of rotenone in the serum.

NaHS was used as an H<sub>2</sub>S donor. When NaHS is dissolved in water, HS<sup>-</sup> is released and forms H<sub>2</sub>S with H<sup>+</sup>. This provides a solution of H<sub>2</sub>S at a concentration that is about 33% of the original concentration of NaHS (Reiffenstein et al., 1992). A most recent study reported that sulfide is rapidly removed from the plasma *in vivo* but remains in both Krebs's and HEPES buffer *in vitro* in a recirculated system (Whitfield et al., 2008). Therefore, we also examined the concentration of sulfide over time after NaHS (100 μM) was added into Krebs's culture solution (in mM: 115 NaCl, 2.5 KCl, 2.46 MgSO<sub>4</sub>, 2 CaCl<sub>2</sub>, 5.6 glucose, 1.38 NaH<sub>2</sub>PO<sub>4</sub>, and 25 NaHCO<sub>3</sub>, pH 7.4) for SH-SY5Y cells. We found that sulfide decayed very fast to an undetectable level after incubation in a petri dish for 30 min in the CO<sub>2</sub> incubator (Figure 1).

MOL #47985

Cell culture and treatment. SH-SY5Y cells from the American Type Culture Collection (ATCC) were cultured in Dulbecco's modified Eagle's medium (Gibco) supplemented with 10% (v/v) FBS, 0.05 U/ml penicillin, 0.05 mg/ml streptomycin and maintained at 37°C with 95% humidified air and 5% CO<sub>2</sub>.

Cells were usually seeded into 60-mm diameter dishes (except for cytochrome *c* release assay) and incubated overnight. For MAPK (*i.e.* p38 and JNK) western blot analysis, regular culture medium was replaced with low-serum media 2 h prior to rotenone treatment in order to minimize background kinase activity. For other experiments, regular medium was changed immediately before treatment. Treatment groups include: (1) control: cells were treated with vehicle (DMSO); (2) rotenone group: cells were treated with 100 nM rotenone alone for 24 h; (3) H<sub>2</sub>S + rotenone group: cells were pretreated with NaHS at indicated concentrations for 30 min prior to rotenone treatment for further 24 h; (4) 5-HD + H<sub>2</sub>S + rotenone group: 5-HD (200 μM) were added into cell culture 15 min before NaHS application, followed by rotenone treatment.

Total sulfide measurement. The procedures are essentially described in the literature with modifications (Gilboa-Garber, 1971). Briefly, aliquots (500 μl) of culture solution (Kreb's buffer) were mixed with trichloroacetic acid (10% w/v, 250 μl), zinc acetate (1% w/v, 250 μl), *N,N*-dimethyl-*p*-phenylenediamine sulphate (20 μM; 133 μl) in 7.2 M HCl and FeCl<sub>3</sub> (30 μM; 133 μl) in 1.2 M HCl in parafilm-enveloped Eppendoff tubes. After 15 min, this mixture was centrifuged at 4,000 g for 10 min. The supernatant was collected and its absorbance measured in 96-well plates at a wavelength of 670 nm. All samples were assayed in duplicate and calculated against a calibration curve of NaHS dissolved in

MOL #47985

Kreb's buffer (in mM): 115 NaCl, 2.5 KCl, 2.46 MgSO<sub>4</sub>, 2 CaCl<sub>2</sub>, 5.6 glucose, 1.38 NaH<sub>2</sub>PO<sub>4</sub>, and 25 NaHCO<sub>3</sub>, pH 7.4 .

Cell viability assay. Cell viability was evaluated with the MTT method as described previously with modifications (Hu et al., 2005). Briefly, the medium was changed before the assay. MTT dissolved in PBS (pH 7.4) was added to the culture media to reach a final concentration of 0.5 mg/ml. After incubation at 37°C for 4 h, the culture media containing MTT were removed. DMSO was then added into each well and the absorbance at 570 nm was measured.

Quantification of apoptosis. To visualize nuclear morphology, cells were fixed in 4% paraformaldehyde and stained with 2.5 µg/ml DNA dye Hoechst 33342. Uniformly stained nuclei were scored as healthy, viable cells. Condensed or fragmented nuclei were scored as apoptotic. In order to obtain unbiased counting, petri dishes were coded and cells were scored blind without knowledge of their prior treatment.

Assessment of mitochondrial membrane potential ( $\Delta\Psi_m$ ) loss.  $\Delta\Psi_m$  was detected with fluorescent probe JC-1 (Sigma, St. Louis, MO), which exists predominantly in monomeric form in cells with depolarized mitochondria and displays fluoresced green at 490 nm. Cells with polarized mitochondria predominantly contain JC-1 in aggregate form and show fluorescence of reddish–orange color. Loading was done by incubating SH-SY5Y cells with 2 µM of JC-1 for 15 min, rinsed twice with PBS, and visualized by a lab-graded Nikon Optical TE2000-S inverted fluorescence microscope with excitation at



MOL #47985

488 nm and emission at >520 nm. Six photos were randomly taken from each well. Fluorescence intensity of the red/green ratio was semi quantitatively determined using Image J software. A decrease in this ratio was interpreted as loss of  $\Delta\Psi_m$ , whereas an increase in the ratio was interpreted as gain in  $\Delta\Psi_m$ .

Western blot analysis. Cells were washed twice with chilled PBS and solubilised in RIPA lysis buffer (Cell signaling). Protein concentrations were determined by Lowry's method. Protein samples were separated by 12-15% SDS/PAGE and transferred on to a nitrocellulose membrane (Amersham Biosciences). After blocking at room temperature in 10% milk in TBST buffer (10 mM Tris-HCl, 120 mM NaCl, 0.1% Tween-20, pH 7.4) for 1 h, the membrane was incubated with various primary antibodies at 4 °C overnight. Membranes were then washed three times in TBST buffer, followed by incubation with 1:10000 dilutions of HRP-conjugated anti-rabbit IgG at room temperature for 1 h, and washed three times in TBST. Visualization was carried out using an ECL® (enhanced chemiluminescence) kit (GE healthcare, UK). The density of the bands on Western blots was quantified by densitometry analysis of the scanned blots using ImageQuant software. The relative phosphorylation was normalized to total protein.

Analysis of cytosolic cytochrome c accumulation. Cells were seeded in 10-cm-diameter dishes at  $8 \times 10^5$  cells/dish and incubated overnight. Cytochrome *c* release from mitochondria into the cytosol was measured by western blot analysis. Briefly, cells were washed twice with chilled PBS and added with 400  $\mu$ l lysis buffer containing 250 mM sucrose, 20 mM HEPES-KOH, pH 7.4, 10 mM KCl, 1.5 mM Na-EGTA, 1.5 mM Na-

MOL #47985

EDTA, 1 mM MgCl<sub>2</sub>, 1 mM dithiothreitol, and a cocktail of protease inhibitors (Boehringer-Mannheim). After incubation on ice for 5 min, the cells were gently scraped off and centrifuged at 1,000 g for 10 min at 4°C. The supernatants were further centrifuged at 16,000 g for 25 min at 4°C. The supernatant was collected as cytosolic fraction and subjected to western blot analysis as mentioned above.

Caspase-9 activity assay. Cells were lysed with chilled lysis buffer followed by centrifugation for 1 min at 10,000 g and the supernatant (cytosolic extract) was determined with a commercial caspase-9 assay kit according to the manufacturer's instructions (BioVision). The fold increase in activity was calculated as the ratio between values obtained from treated samples versus those obtained in untreated controls.

Statistical analysis. All data were presented as mean ± SEM. Statistical significance was assessed with one-way analysis of variance (ANOVA) followed by a post hoc (Bonferroni) test for multiple group comparison. Differences with *p* value less than 0.05 were considered statistically significant.

## Results

### H<sub>2</sub>S Suppresses Rotenone-Induced Cytotoxicity and Apoptosis

To determine the effect of H<sub>2</sub>S on the pro-apoptotic activity of rotenone, SH-SY5Y cells were treated with rotenone (100 nM, 24 h) in the absence or presence of NaHS, a donor of H<sub>2</sub>S. As shown in Figure 2, rotenone substantially decreased cell viability by 43% as compared to that of control. The effect of rotenone was attenuated by NaHS at

MOL #47985

concentrations from 1 to 300  $\mu\text{M}$ , indicating that  $\text{H}_2\text{S}$  produced protective effects against rotenone-induced cell injury. Treatment with NaHS alone (up to 300  $\mu\text{M}$ ) did not show any effect on cell viability (data not shown).

The beneficial effects of  $\text{H}_2\text{S}$  against rotenone-induced apoptosis were further examined by Hoechst 33342 staining assay. Representative photomicrographs of nuclei morphology of SH-SY5Y cells were shown in Figure 3a-c. Treatment with rotenone induced condensed and fragmented nuclei, a characteristic of apoptosis. NaHS at 100  $\mu\text{M}$  significantly attenuated this effect (Figure 3c). Figure 3d shows that NaHS (1-300  $\mu\text{M}$ ) concentration-dependently attenuated the pro-apoptotic activity of rotenone ( $\text{IC}_{50}$  = approximate 55  $\mu\text{M}$ ). This confirms the protective effects of NaHS against rotenone-induced apoptosis in SH-SY5Y cells.

### $\text{H}_2\text{S}$ Prevents Rotenone-Induced $\Delta\Psi_m$ Loss and Inhibits Cytochrome *c* Release

To investigate the mechanisms for the protective effects of NaHS on rotenone-induced apoptosis,  $\Delta\Psi_m$  was determined with molecular probe JC-1. As shown in Figure 4a and quantified in Figure 4b, as a result of rotenone treatment for 9 h, cells displayed a loss or collapse of  $\Delta\Psi_m$ , indicated by a shift from red-orange to greenish yellow fluorescence. Pretreatment with NaHS (100  $\mu\text{M}$ ) significantly prevented the loss of  $\Delta\Psi_m$  in the cells. These findings suggest that cytoprotection by  $\text{H}_2\text{S}$  may be mediated by raising cellular resistance against the initiating steps of apoptosis, namely the decrease of  $\Delta\Psi_m$ . In addition, western blot analysis revealed that significant amounts of cytochrome *c* were released from mitochondria into the cytosol in rotenone-treated cells. NaHS (100  $\mu\text{M}$ ), which itself had no significant effect, attenuated the stimulatory effect of rotenone

MOL #47985

on cytochrome *c* release (Figure 4c). These findings indicate that NaHS may produce anti-apoptotic effects via the preservation of mitochondrial function.

### H<sub>2</sub>S Reverses Rotenone-Induced Changes of Bax and Bcl-2 Levels in SH-SY5Y Cells

Bcl-2, an anti-apoptotic protein, prevents the release of cytochrome *c* from mitochondria, whereas Bax, a pro-apoptotic protein, promotes its release. During apoptosis, Bax translocates to the outer mitochondria membrane to induce mitochondrial membrane permeabilization. This process is blocked by Bcl-2 protein. Therefore, the effects of NaHS on the protein levels of Bcl-2 and Bax were also examined. Rotenone-induced changes of protein levels of Bcl-2 and Bax in the presence and absence of NaHS (Figure 5). Densitometric analysis indicates that rotenone significantly decreased the basal level of Bcl-2, but increased the Bax protein expression (Figure 5a). The ratio of Bcl-2 over Bax was decreased by 40% in rotenone-treated cells (Figure 5b). This effect was markedly attenuated by NaHS (100  $\mu$ M).

### H<sub>2</sub>S Decreases Rotenone-Induced Caspase-9/3 Activation and PARP Cleavage

The cytochrome *c*, together with Apaf-1 and pro-caspase-9, may form apoptosome which activates caspase-9 and its downstream caspase cascades. It was found that rotenone increased the caspase-9 activity by 2.5 fold when compared to that of control group. This increase was attenuated by NaHS (100  $\mu$ M) (Figure 6a). Caspase-3 is a critical executioner of apoptosis and the pro-caspase-3 can be cleaved by active caspase-9. As shown in Figure 6b, treatment of the cells with rotenone significantly induced the cleavage of procaspase-3 (35 kD) to its 19- and 17-kD subunits, which was dramatically

MOL #47985

inhibited by NaHS (100  $\mu$ M). Our data suggest that rotenone did activate caspase-3 in SH-SY5Y cells and that this activation could be suppressed by NaHS.

Poly (ADP-ribose) polymerase (PARP) is an enzyme implicated in DNA damage and repair mechanisms. Cleavage of PARP by active caspase-3 from native 116 kD to 89 kD is a hallmark of apoptosis. We then examined the effect of H<sub>2</sub>S on rotenone-induced apoptosis in SH-SY5Y cells by measuring PARP cleavage using western blot analysis. As shown in Figure 6c, treatment with rotenone increased the cleavage of PARP by 3.8 fold in SH-SY5Y cells. Pretreatment with NaHS (10-300  $\mu$ M) for 30 min significantly reduced PARP cleavage induced by rotenone in a concentration-dependent manner (Figure 6c).

#### The Protective Effects of H<sub>2</sub>S Involves mitoK<sub>ATP</sub> channels

To examine the involvement of mitoK<sub>ATP</sub> channels, 5-HD (200  $\mu$ M), a selective mitoK<sub>ATP</sub> channel blocker, was given 15 min before NaHS application. Interestingly, 5-HD, which had no effect by itself, significantly attenuated the inhibitory effects of NaHS on rotenone-induced cytochrome *c* release, caspase-9 activity, cell injury and PARP cleavage (Figure 7a-d). These data suggest that the initial exposure to NaHS resulted in the opening of mitoK<sub>ATP</sub> channels located in inner mitochondrial membrane, which in turn, mediate the subsequent signaling cascade leading to the observed neuroprotective effects.

#### Rotenone Induces p38/JNK MAPK Activation

Both P38 and JNK signaling pathways are critical for the degeneration of dopaminergic neuronal cells (Newhouse et al., 2004). We therefore further studied the

MOL #47985

contribution of MAPK to the neuroprotective effects of H<sub>2</sub>S. It was found that phosphorylation of p38 MAPK occurred as early as 5 min and reached the peak at 15 min after rotenone treatment. This effect gradually reduced and disappeared by 4 h after treatment (Figure 8a). Rotenone also induced the phosphorylation of JNK but with a slower time course. The peak effect occurred at 4 h and almost disappeared by 24 h after treatment (Figure 8b).

In addition, SB203580 (a p38 MAPK inhibitor) and SP600125 (a selective JNK inhibitor) markedly attenuated rotenone-induced cell injury (Figure 8c) and apoptosis (Figure 8d) in SH-SY5Y cells. These data further confirmed that both p38 and JNK MAPK are involved in the mediation of the effects of rotenone.

### H<sub>2</sub>S Attenuates Rotenone-Induced p38/JNK MAPK Activation

To study the signaling mechanisms of the neuroprotective effects of H<sub>2</sub>S, the concentration-dependent effects of H<sub>2</sub>S on rotenone-induced stimulation of p38/JNK MAPK were also studied. As shown in Figure 9, the maximal effects of rotenone on the phosphorylation of both p38 (at 15 min, Figure 9a) and JNK (at 4 h, Figure 9b) were attenuated by NaHS (1-300 μM) in a concentration-dependent manner. These data strongly suggest that the anti-apoptotic effects of NaHS are associated with inhibition of the p38/JNK signaling pathways.

## **Discussion**

Rotenone is a naturally occurring toxin and a commonly used pesticide to reproduce the neurochemical, neuropathological and behavioural features of PD in rats. In the

MOL #47985

present study, we demonstrated for the first time that NaHS was able to inhibit rotenone-mediated cytotoxicity and apoptosis in a concentration-dependent manner. The underlying mechanisms may be associated with suppression of rotenone-induced events including  $\Delta\Psi_m$  loss, release of cytochrome *c* and activation of subsequent caspase cascades via regulation of mitoK<sub>ATP</sub> channels/ p38- & JNK-MAPK pathway (Figure 10).

Mitochondrial dysfunction is a prominent feature in apoptosis (Lemasters et al., 2002). Rotenone is a complex I inhibitor. The inhibition of complex I may induce  $\Delta\Psi_m$  loss and the release of pro-apoptotic proteins (*e.g.* cytochrome *c*) from the mitochondrial intermembrane space to cytosol, where cytochrome *c* forms oligomeric complex with Apaf-1 and activates caspase-9. Our data showed that H<sub>2</sub>S prevented rotenone-induced  $\Delta\Psi_m$  loss and cytosolic accumulation of cytochrome *c*, suggesting that H<sub>2</sub>S may produce neuroprotective effects via preservation of mitochondrial function. The increased mitochondrial permeabilization and release of cytochrome *c* may also be regulated by pro-apoptotic proteins, such as Bax. In apoptotic cells, Bax interacts with Bid and the resultant conformational change causes Bax to translocate from cytoplasm to the mitochondria, where it promotes the opening of permeability transition pore and thereby mediates the efflux of cytochrome *c*. This process could be blocked by mitochondrial protein Bcl-2. Hence, the ratio of Bcl-2/Bax may be used to indicate mitochondrial permeability. Consistent with previous findings (De Sarno et al., 2003), we found that rotenone decreased the ratio of Bcl-2/Bax protein in SH-SY5Y cells. This effect was significantly attenuated by H<sub>2</sub>S. Thus, the protective effects of H<sub>2</sub>S on mitochondrial function may also occur via suppression of the expression of the pro-apoptotic proteins.

MOL #47985

The release of cytochrome *c* and apoptosis-inducing factor (AIF) from mitochondria to cytosol may further stimulate caspase-9, which may lead to the activation of caspase-3 and subsequent degradation of cellular death substrates (*e.g.* PARP). We found in the present study that NaHS attenuated the effects of rotenone on caspase-9/3 activation and PARP degradation and therefore protected cells against apoptotic injury. The effects of NaHS on this signaling cascade may be derived from the preservation of mitochondrial function via prevention of  $\Delta\Psi_m$  loss and inhibition of cytochrome *c* release.

Similar to the findings by (Whitfield et al., 2008), we found that H<sub>2</sub>S concentration decayed rapidly (within 30 min) in the culture solution. Therefore, it appeared that H<sub>2</sub>S level was reaching undetectable levels before the addition of rotenone in our present experimental setting. So the obvious question is how H<sub>2</sub>S may protect cells against rotenone-induced injury. Recent studies suggested that H<sub>2</sub>S plays a critical role in opening K<sub>ATP</sub> channels (Dawe et al., 2008; Wang, 2002; Yang et al., 2005) which contributes to neuroprotective effects (Busija et al., 2004; Wu et al., 2006). The role of K<sub>ATP</sub> channels in PD has been addressed as well. Activation of mitoK<sub>ATP</sub> channel protects against rotenone-induced cell death and neurochemical alterations in rats (Tai et al., 2003; Zhou et al., 2007). By examining the involvement of mitoK<sub>ATP</sub> channels in the neuroprotective effects of H<sub>2</sub>S, we found that blockade of mitoK<sub>ATP</sub> channels with 5-HD attenuated the protective effects of H<sub>2</sub>S on rotenone-induced cell apoptosis. These findings suggest that H<sub>2</sub>S rapidly opens mitoK<sub>ATP</sub> channels which, in turn, trigger a series of persistent intracellular responses, including inhibition of MAPK signaling pathway and preservation of mitochondrial integrity (Zhang et al., 2007). This triggering effect of



MOL #47985

H<sub>2</sub>S may be similar to the mechanism for the cardioprotection conferred by H<sub>2</sub>S preconditioning (Pan et al., 2008). Interestingly, it was also reported that H<sub>2</sub>S can be rapidly absorbed in a kind of sulfur store in a form of bound sulfane sulfur and then gradually released upon stimulation (Ogasawara et al., 1993; Warenycia et al., 1990). Therefore, this may also explain the persistent protective effects of H<sub>2</sub>S despite its short half-life.

Stimulation of MAPK (*i.e.* ERK1/2, p38 and JNK) leads to a wide range of cellular responses, including growth, differentiation, inflammation and apoptosis. As rotenone only stimulates the activities of JNK and p38, but not that of ERK1/2, in SH-SY5Y cells (Newhouse et al., 2004), we therefore only investigated the role of H<sub>2</sub>S in rotenone-induced phosphorylation of p38 and JNK in the present study. We found that H<sub>2</sub>S concentration-dependently inhibited the activation of these two kinases. The involvement of p38 MAPK in the neuroprotective effects has also been reported by our and other groups. Rinaldi *et al* found that H<sub>2</sub>S promotes the survival of the human polymorphonuclear cells via inhibition of p38 and caspase-3 (Rinaldi et al., 2006). We recently reported that H<sub>2</sub>S attenuates LPS-stimulated p38 activation in microglial cells (Hu et al., 2007). All these findings indicate that inhibition of p38 may contribute to the protective effects of H<sub>2</sub>S. Since p38 MAPK was shown to mediate pro-apoptotic protein Bax-induced mitochondrial membrane permeabilization and neuronal apoptosis (Gomez-Lazaro et al., 2007), the anti-apoptotic effect of H<sub>2</sub>S may be associated with the suppression of the activation of both p38 and JNK MAPK caused by rotenone.

The glutathione (GSH) redox cycle is a major endogenous protective system and an important component of the antioxidant machinery of the nervous system (Seyfried et al.,

MOL #47985

2000). Recent evidence indicates that depletion of cellular GSH results in the accumulation of ROS and loss of mitochondrial function (Bharat et al., 2002). Rotenone also induces the depletion of intracellular GSH and the accumulation of ROS, which in turn activates p38/JNK MAPK in the cells. It has been previously demonstrated that H<sub>2</sub>S protects neuronal cells against oxidative stress via increasing GSH production (Kimura and Kimura, 2004). It is therefore logically to expect that GSH also contributes to the anti-apoptotic effects of H<sub>2</sub>S on rotenone-treated SH-SY5Y cells, but more experiments are warranted to further confirm this hypothesis.

In conclusion, the present observations identify a beneficial role of H<sub>2</sub>S against rotenone-induced apoptosis in SH-SY5Y cells via regulation of mitoK<sub>ATP</sub> channels and inhibition of p38 & JNK pathway. As epidemiological studies have revealed a correlation between general pesticide (*i.e.* rotenone) exposure and increased risk for PD, our findings may therefore provide a potential venue to treat PD.

**Acknowledgements:** The authors thank Miss Ester Khin Sandar Win for technical support.

MOL #47985

## References

- Abe K and Kimura H (1996) The possible role of hydrogen sulfide as an endogenous neuromodulator. *J Neurosci* **16**(3):1066-1071.
- Bharat S, Cochran BC, Hsu M, Liu J, Ames BN and Andersen JK (2002) Pre-treatment with R-lipoic acid alleviates the effects of GSH depletion in PC12 cells: implications for Parkinson's disease therapy. *Neurotoxicology* **23**(4-5):479-486.
- Busija DW, Lacza Z, Rajapakse N, Shimizu K, Kis B, Bari F, Domoki F and Horiguchi T (2004) Targeting mitochondrial ATP-sensitive potassium channels--a novel approach to neuroprotection. *Brain Res Brain Res Rev* **46**(3):282-294.
- Dawe GS, Han SP, Bian JS and Moore PK (2008) Hydrogen sulphide in the hypothalamus causes an ATP-sensitive K<sup>+</sup> channel-dependent decrease in blood pressure in freely moving rats. *Neuroscience* **152**(1):169-177.
- De Sarno P, Shestopal SA, King TD, Zmijewska A, Song L and Jope RS (2003) Muscarinic receptor activation protects cells from apoptotic effects of DNA damage, oxidative stress, and mitochondrial inhibition. *J Biol Chem* **278**(13):11086-11093.
- Eto K, Asada T, Arima K, Makifuchi T and Kimura H (2002a) Brain hydrogen sulfide is severely decreased in Alzheimer's disease. *Biochem Biophys Res Commun* **293**(5):1485-1488.
- Eto K, Ogasawara M, Umemura K, Nagai Y and Kimura H (2002b) Hydrogen sulfide is produced in response to neuronal excitation. *J Neurosci* **22**(9):3386-3391.
- Fleming SM, Zhu C, Fernagut PO, Mehta A, DiCarlo CD, Seaman RL and Chesselet MF (2004) Behavioral and immunohistochemical effects of chronic intravenous and subcutaneous infusions of varying doses of rotenone. *Exp Neurol* **187**(2):418-429.
- Gilboa-Garber N (1971) Direct spectrophotometric determination of inorganic sulfide in biological materials and in other complex mixtures. *Anal Biochem* **43**(1):129-133.
- Gomez-Lazaro M, Galindo MF, Melero-Fernandez de Mera RM, Fernandez-Gomez FJ, Concannon CG, Segura MF, Comella JX, Prehn JH and Jordan J (2007) Reactive oxygen species and p38 mitogen-activated protein kinase activate Bax to induce mitochondrial cytochrome c release and apoptosis in response to malonate. *Mol Pharmacol* **71**(3):736-743.
- Hu LF, Wang S, Shi XR, Yao HH, Sun YH, Ding JH, Liu SY and Hu G (2005) ATP-sensitive potassium channel opener iptakalim protected against the cytotoxicity of MPP<sup>+</sup> on SH-SY5Y cells by decreasing extracellular glutamate level. *J Neurochem* **94**(6):1570-1579.
- Hu LF, Wong PT, Moore PK and Bian JS (2007) Hydrogen sulfide attenuates lipopolysaccharide-induced inflammation by inhibition of p38 mitogen-activated protein kinase in microglia. *J Neurochem* **100**(4):1121-1128.
- Kimura H (2000) Hydrogen sulfide induces cyclic AMP and modulates the NMDA receptor. *Biochem Biophys Res Commun* **267**(1):129-133.
- Kimura H (2002) Hydrogen sulfide as a neuromodulator. *Mol Neurobiol* **26**(1):13-19.
- Kimura Y and Kimura H (2004) Hydrogen sulfide protects neurons from oxidative stress. *Faseb J* **18**(10):1165-1167.

MOL #47985

- Lee SW, Hu YS, Hu LF, Lu Q, Dawe GS, Moore PK, Wong PT and Bian JS (2006) Hydrogen sulphide regulates calcium homeostasis in microglial cells. *Glia* **54**(2):116-124.
- Lemasters JJ, Qian T, He L, Kim JS, Elmore SP, Cascio WE and Brenner DA (2002) Role of mitochondrial inner membrane permeabilization in necrotic cell death, apoptosis, and autophagy. *Antioxid Redox Signal* **4**(5):769-781.
- Nagai Y, Tsugane M, Oka J and Kimura H (2004) Hydrogen sulfide induces calcium waves in astrocytes. *Faseb J* **18**(3):557-559.
- Newhouse K, Hsuan SL, Chang SH, Cai B, Wang Y and Xia Z (2004) Rotenone-induced apoptosis is mediated by p38 and JNK MAP kinases in human dopaminergic SH-SY5Y cells. *Toxicol Sci* **79**(1):137-146.
- Ogasawara Y, Ishii K, Togawa T and Tanabe S (1993) Determination of bound sulfur in serum by gas dialysis/high-performance liquid chromatography. *Anal Biochem* **215**(1):73-81.
- Pan TT, Neo KL, Hu LF, Yong QC and Bian JS (2008) H<sub>2</sub>S preconditioning-induced PKC activation regulates intracellular calcium handling in rat cardiomyocytes. *Am J Physiol Cell Physiol* **294**(1):C169-177.
- Qu K, Chen CP, Halliwell B, Moore PK and Wong PT (2006) Hydrogen sulfide is a mediator of cerebral ischemic damage. *Stroke* **37**(3):889-893.
- Qu K, Lee SW, Bian JS, Low CM and Wong PT (2008) Hydrogen sulfide: neurochemistry and neurobiology. *Neurochem Int* **52**(1-2):155-165.
- Reiffenstein RJ, Hulbert WC and Roth SH (1992) Toxicology of hydrogen sulfide. *Annu Rev Pharmacol Toxicol* **32**:109-134.
- Rinaldi L, Gobbi G, Pambianco M, Micheloni C, Mirandola P and Vitale M (2006) Hydrogen sulfide prevents apoptosis of human PMN via inhibition of p38 and caspase 3. *Lab Invest* **86**(4):391-397.
- Seyfried J, Soldner F, Kunz WS, Schulz JB, Klockgether T, Kovar KA and Wullner U (2000) Effect of 1-methyl-4-phenylpyridinium on glutathione in rat pheochromocytoma PC 12 cells. *Neurochem Int* **36**(6):489-497.
- Szabo C (2007) Hydrogen sulphide and its therapeutic potential. *Nat Rev Drug Discov* **6**(11):917-935.
- Tai KK, McCrossan ZA and Abbott GW (2003) Activation of mitochondrial ATP-sensitive potassium channels increases cell viability against rotenone-induced cell death. *J Neurochem* **84**(5):1193-1200.
- Umemura K and Kimura H (2007) Hydrogen sulfide enhances reducing activity in neurons: neurotrophic role of H<sub>2</sub>S in the brain? *Antioxid Redox Signal* **9**(11):2035-2041.
- Wang R (2002) Two's company, three's a crowd: can H<sub>2</sub>S be the third endogenous gaseous transmitter? *Faseb J* **16**(13):1792-1798.
- Warencya MW, Goodwin LR, Francom DM, Dieken FP, Kombian SB and Reiffenstein RJ (1990) Dithiothreitol liberates non-acid labile sulfide from brain tissue of H<sub>2</sub>S-poisoned animals. *Arch Toxicol* **64**(8):650-655.
- Whitfield NL, Kreimier EL, Verdial FC, Skovgaard N and Olson KR (2008) Reappraisal of H<sub>2</sub>S/sulfide concentration in vertebrate blood and its potential significance in ischemic preconditioning and vascular signaling. *Am J Physiol Regul Integr Comp Physiol* **294**(6):R1930-1937.

MOL #47985

- Wu L, Shen F, Lin L, Zhang X, Bruce IC and Xia Q (2006) The neuroprotection conferred by activating the mitochondrial ATP-sensitive K<sup>+</sup> channel is mediated by inhibiting the mitochondrial permeability transition pore. *Neurosci Lett* **402**(1-2):184-189.
- Yang W, Yang G, Jia X, Wu L and Wang R (2005) Activation of KATP channels by H<sub>2</sub>S in rat insulin-secreting cells and the underlying mechanisms. *J Physiol* **569**(Pt 2):519-531.
- Zhang S, Zhou F, Ding JH, Zhou XQ, Sun XL and Hu G (2007) ATP-sensitive potassium channel opener iptakalim protects against MPP-induced astrocytic apoptosis via mitochondria and mitogen-activated protein kinase signal pathways. *J Neurochem* **103**(2):569-579.
- Zhou F, Wu JY, Sun XL, Yao HH, Ding JH and Hu G (2007) Iptakalim alleviates rotenone-induced degeneration of dopaminergic neurons through inhibiting microglia-mediated neuroinflammation. *Neuropsychopharmacology* **32**(12):2570-2580.

MOL #47985

### Footnotes

- This work is supported by research grants from Singapore National Medical Research Council (1057/2006) and Singapore Biomedical Research Council (07/1/21/19/509).

Reprint requests should be sent to: Dr. Bian Jinsong, Department of Pharmacology, Yong Loo Lin School of Medicine, National University of Singapore, Singapore, 117597.

Email: [phcbjs@nus.edu.sg](mailto:phcbjs@nus.edu.sg).

MOL #47985

## Legends for figures

**Figure 1** Colorimetric assay of exogenous sulfide (NaHS) consumption in culture solution (Kreb's buffer) of SH-SY5Y cells. Total NaHS (100  $\mu$ M) was initially added into sterile Krebs buffer for cell culture. The total sulfide levels in culture supernatant at different time points were determined with colorimetric assay. Results show representative time-course of sulfide concentrations of three independent measurements.

**Figure 2** Effects of NaHS on rotenone-induced cytotoxicity in SH-SY5Y cells. Cell viability was determined using MTT method. Values are expressed as the percentage of the untreated control and represented as mean  $\pm$  S.E.M. of at least 5 independent experiments.  $^{\dagger\dagger\dagger}p < 0.001$  vs control;  $^*p < 0.05$ ,  $^{**}p < 0.01$  vs rotenone group, respectively.

**Figure 3** Effects of NaHS on rotenone-induced cell apoptosis in SH-SY5Y cells. Cell apoptosis was detected by Hoechst 33342 staining in cells treated with (a) vehicle, (b) rotenone (100 nM, rot), and (c) NaHS (100  $\mu$ M) + rot. Arrows identify cells with condensed or fragmented nuclei, characteristic of apoptosis. (d) Quantification of apoptosis based on nuclear condensation or fragmentation. Data were expressed as mean  $\pm$  S.E.M. for at least 7 independent experiments.  $^{\dagger\dagger\dagger}p < 0.001$  vs control;  $^*p < 0.05$ ,  $^{**}p < 0.01$ ,  $^{***}p < 0.001$  vs rotenone group, respectively.

**Figure 4** Effects of NaHS on rotenone-induced  $\Delta\Psi_m$  loss and cytochrome c release in SH-SY5Y cells. (a) Representative pictures of the cells stained with JC-1 from different groups. (b) Bar chart shows the quantified data of four independent experiments.

MOL #47985

Quantification of  $\Delta\Psi_m$  expressed as the ratio of J-aggregate to JC-1 monomer (red: green) fluorescence intensity. Data are expressed as mean  $\pm$  S.E.M. (c) Representative immunoblots for cytochrome *c* release from 3 independent experiments. Cytosolic fractions of the extract were subjected to 15% SDS-PAGE and immunoblotted with anti-cytochrome *c* antibody.  $\beta$ -actin was used as a control for equal loading.  $^{\dagger\dagger\dagger}p<0.001$  vs control;  $^{**}p<0.01$  vs rotenone group.

**Figure 5** Effects of NaHS on rotenone-induced alterations of Bcl-2 and Bax level in SH-SY5Y cells. Total proteins extracts were subjected to 15% SDS-PAGE for western blot analysis. (a) Representative images from four different experiments. Tubulin was used as a loading control. (b) Densitometric analysis performed by normalizing Bcl-2 proteins to Bax proteins signals. Data were expressed as the mean  $\pm$  S.E.M.  $^{\dagger}p<0.05$  vs control;  $^{*}p<0.05$  vs rotenone group.

**Figure 6** Effects of NaHS on rotenone-induced caspase-3/9 activation and PARP cleavage in SH-SY5Y cells. (a) Mean data showing NaHS attenuated rotenone (rot) induced caspase-9 activation. Results are normalized by the control values. (b & c) The levels of cleaved caspase-3 (b) and PARP (c) were determined by western blot. Data was expressed by the ratio of cleaved PARP over total (uncleaved plus cleaved) PARP. Tubulin and  $\beta$ -actin were used as controls for equal loading. Mean  $\pm$  S.E.M.; n=4-8 independent experiments.  $^{\dagger\dagger\dagger}p<0.001$  vs control;  $^{*}p<0.05$ ,  $^{**}p<0.01$ ,  $^{***}p<0.001$  vs rotenone group respectively.



MOL #47985

**Figure 7** Effect of mitoK<sub>ATP</sub> channels blocker 5-HD on the protective effects of NaHS against rotenone-induced cytochrome c release (a), caspase-9 activation (b), cell injury (c) and PARP cleavage (d) in SH-SY5Y cells. Cells were pretreated with NaHS for 30 min prior to rotenone treatment for 24 h. 5-HD (200  $\mu$ M) was added into cells before NaHS treatment. Data are presented as the percentage of control value and expressed as mean  $\pm$  S.E.M.  $\dagger\dagger$   $p < 0.01$ ,  $\dagger\dagger\dagger$   $p < 0.001$  vs control; \*  $p < 0.05$ , \*\*  $p < 0.01$ , \*\*\*  $p < 0.001$  vs rotenone group; #  $p < 0.05$ , ##  $p < 0.01$  vs NaHS + rotenone group.

**Figure 8** Rotenone stimulates both p38 & JNK MAPK in SH-SY5Y cells. (a & b) Time course for the effects of rotenone on phosphorylation of p38 (a) and JNK (b). (c & d) Blockade of p38 MAPK with SB203580 (10  $\mu$ M) and JNK with SP600125 (10  $\mu$ M) attenuated rotenone-induced cell injury assayed by MTT method (c) and PARP cleavage (d). Data are presented as the percentage of control value and expressed as mean  $\pm$  S.E.M.  $\dagger\dagger\dagger$   $p < 0.001$  vs control; \*  $p < 0.05$ , \*\*  $p < 0.01$ , \*\*\*  $p < 0.001$  vs rotenone group respectively.

**Figure 9** Concentration-dependent effects of NaHS (0.1-300  $\mu$ M) on rotenone-induced activation of p38 (a) & JNK (b) MAPK in SH-SY5Y cells. Data are presented as mean  $\pm$  S.E.M. of 6 independent experiments.  $\dagger\dagger\dagger$   $p < 0.001$  vs control; \*  $p < 0.05$ , \*\*  $p < 0.01$  vs rotenone group respectively.

**Figure 10** Proposed signaling mechanisms for the effects of H<sub>2</sub>S on rotenone-induced apoptosis. Rotenone induces complex I inhibition which initiates the dissipation of  $\Delta\Psi_m$ , causing the matrix swelling and promoting the opening of mitochondrial permeability

MOL #47985

transition pore. Rotenone may also stimulate intracellular p38/JNK MAPK pathway. The activation of p38/JNK MAPK, in turn, induces the recruitment of cytoplasmic apoptotic members of Bcl-2 family proteins (e.g. Bax, Bid) to mitochondria and forms permeability transition pore, causing the release of cytochrome *c* to cytosol. The cytosolic apoptotic executors (cytochrome *c*, Apaf-1 and pro-caspase-9) form apoptosome which lead to activation of pro-caspase-9, subsequently activating caspase-3. The mechanisms underlying the anti-apoptotic effects of H<sub>2</sub>S may result from opening of mitoK<sub>ATP</sub> channels, which in turn mediates the prevention of  $\Delta\Psi_m$  loss and the inhibition of p38/JNK MAPK pathway.

Figure 1

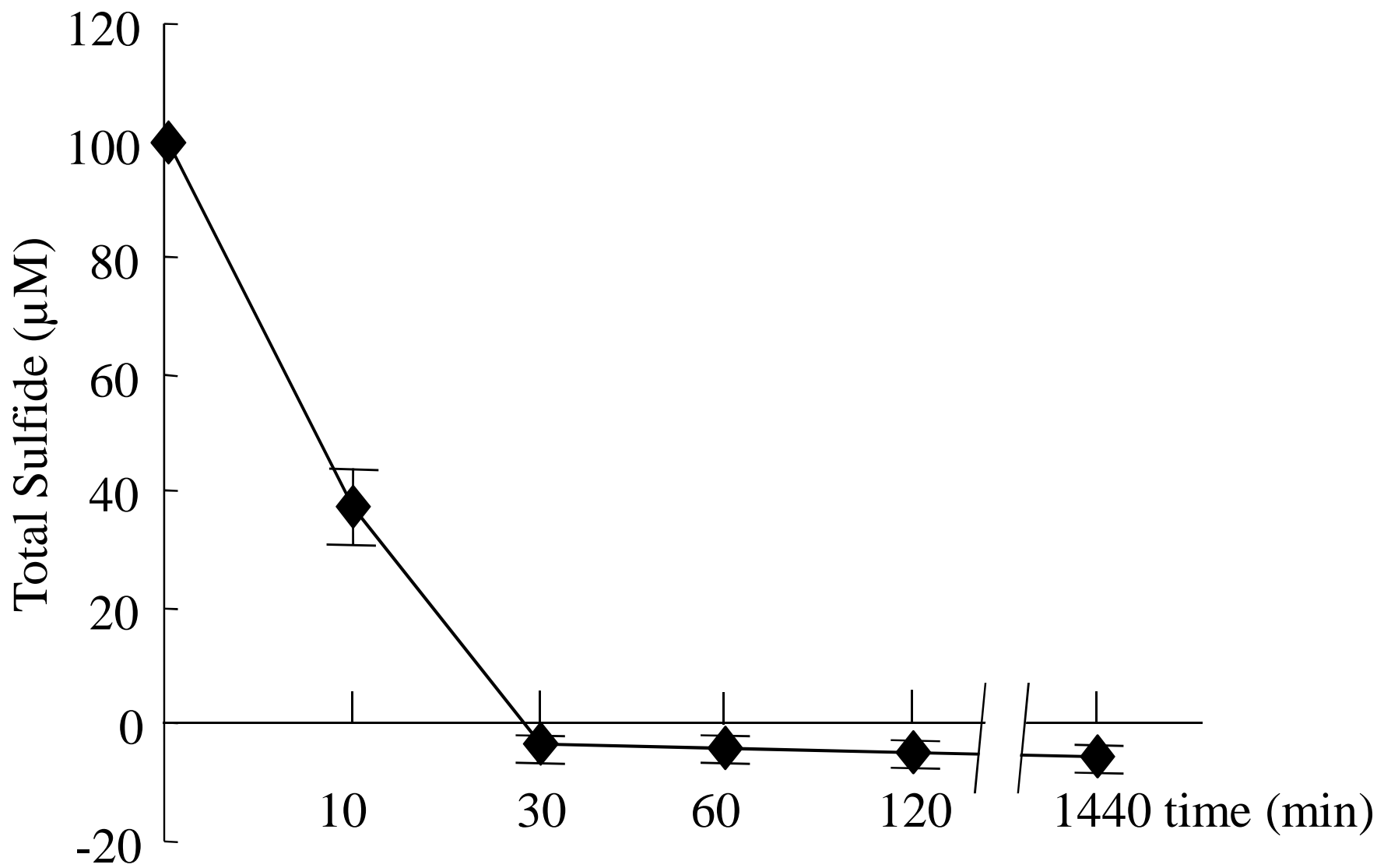


Figure 2

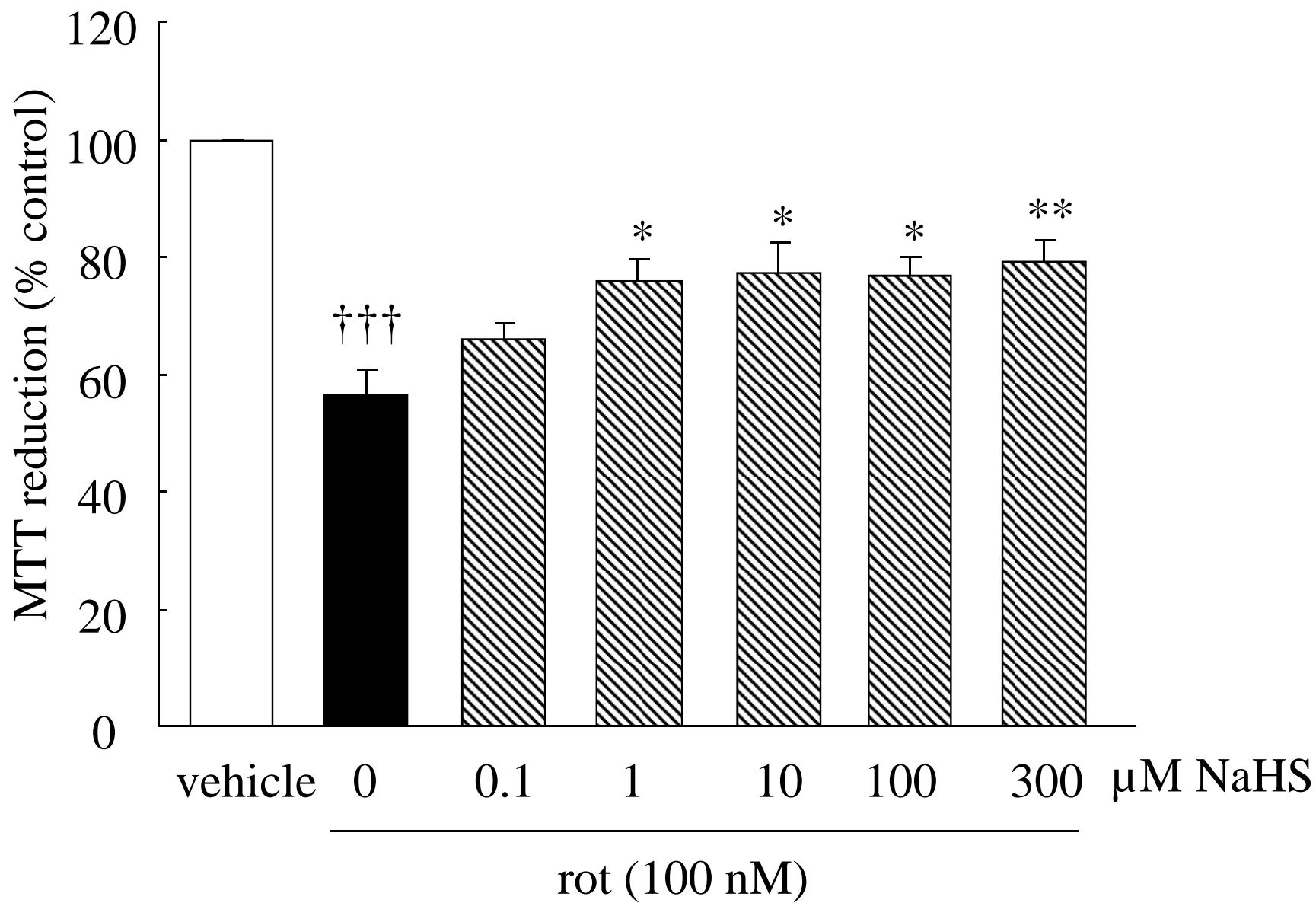


Figure 3

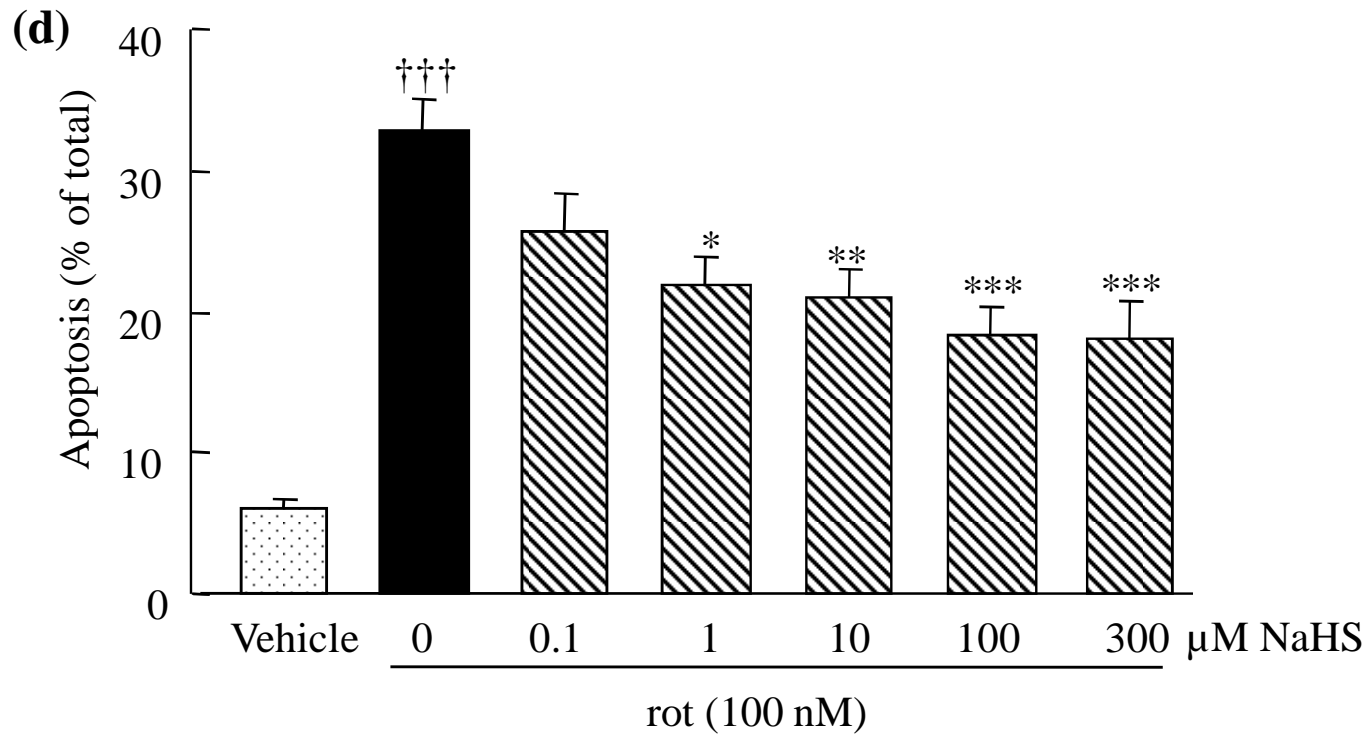
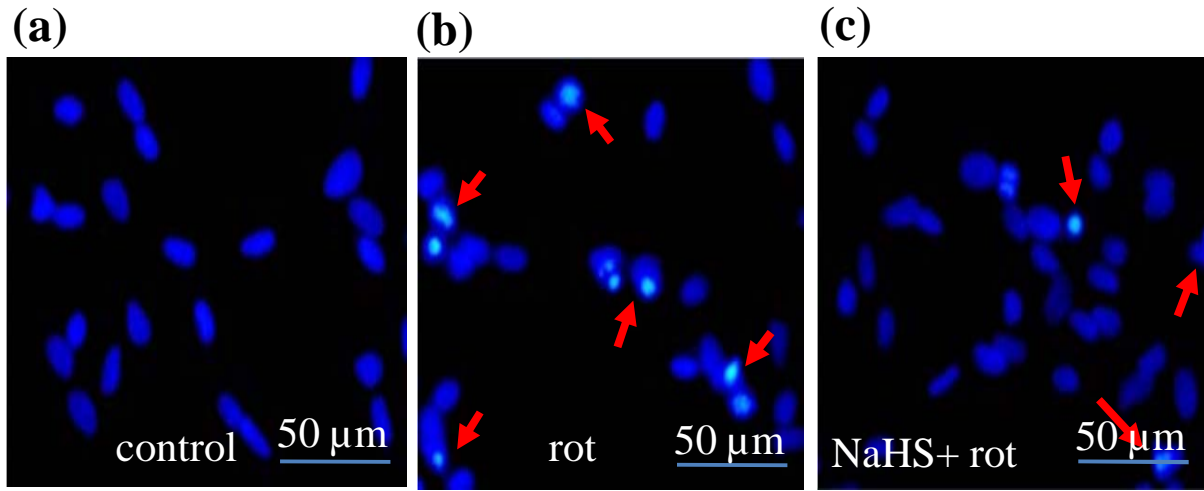


Figure 4

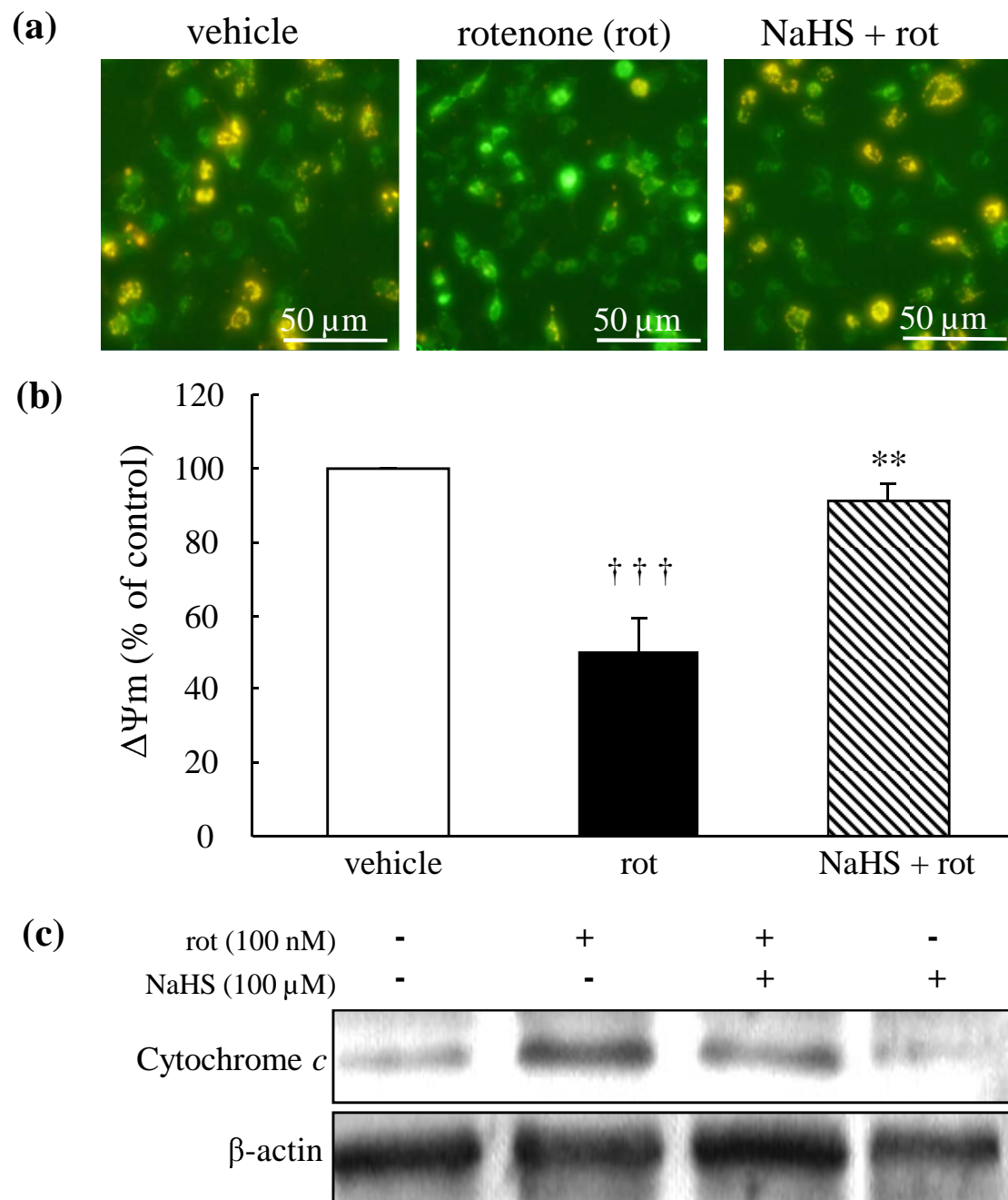


Figure 5

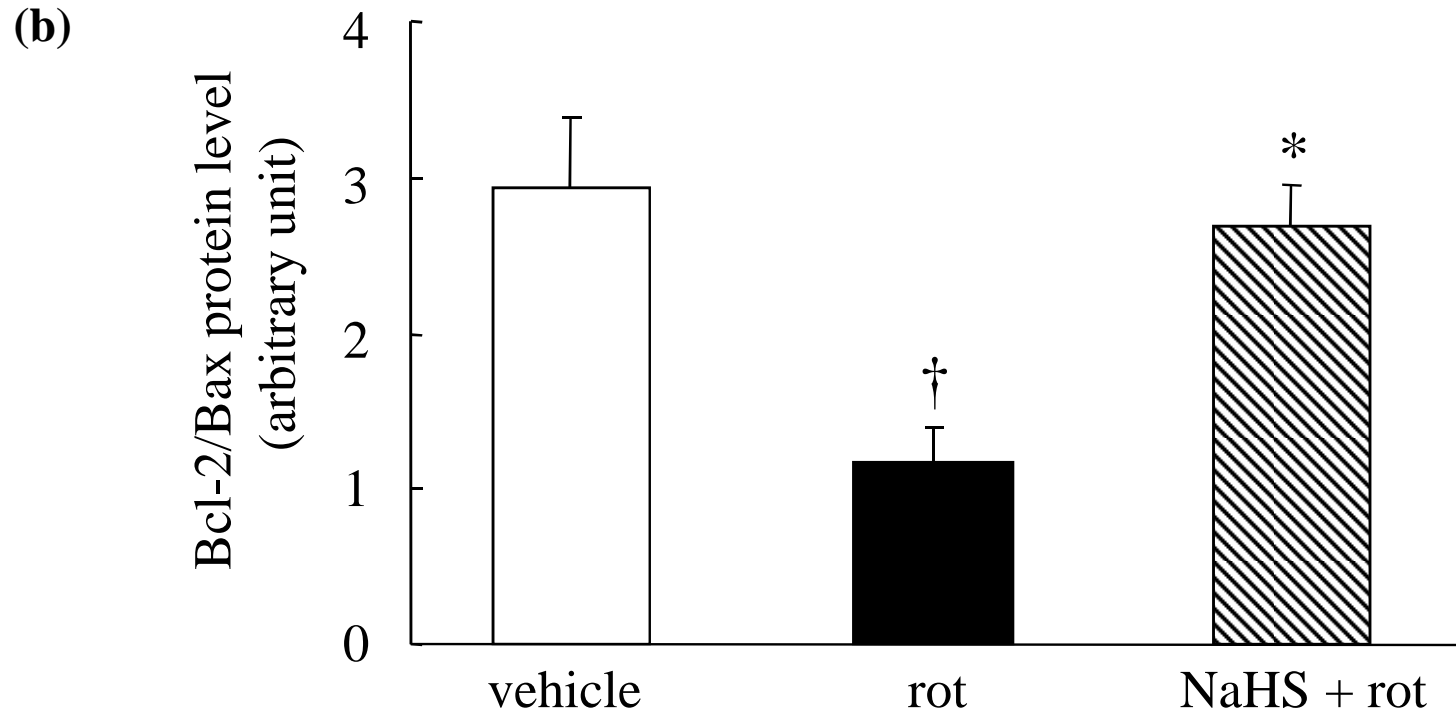
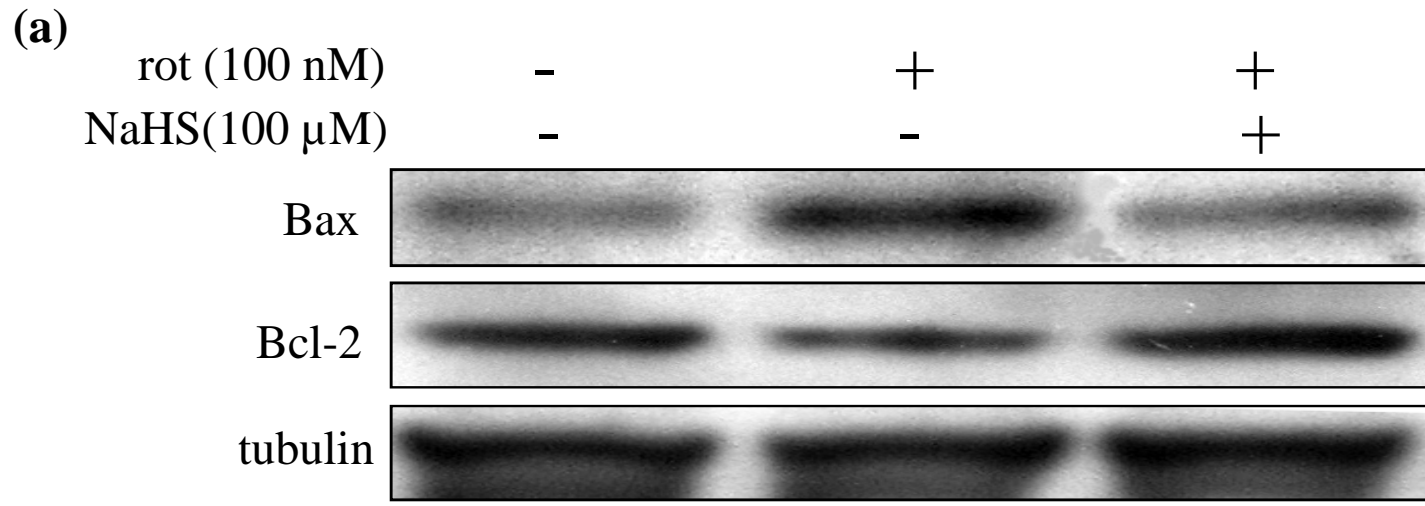


Figure 6

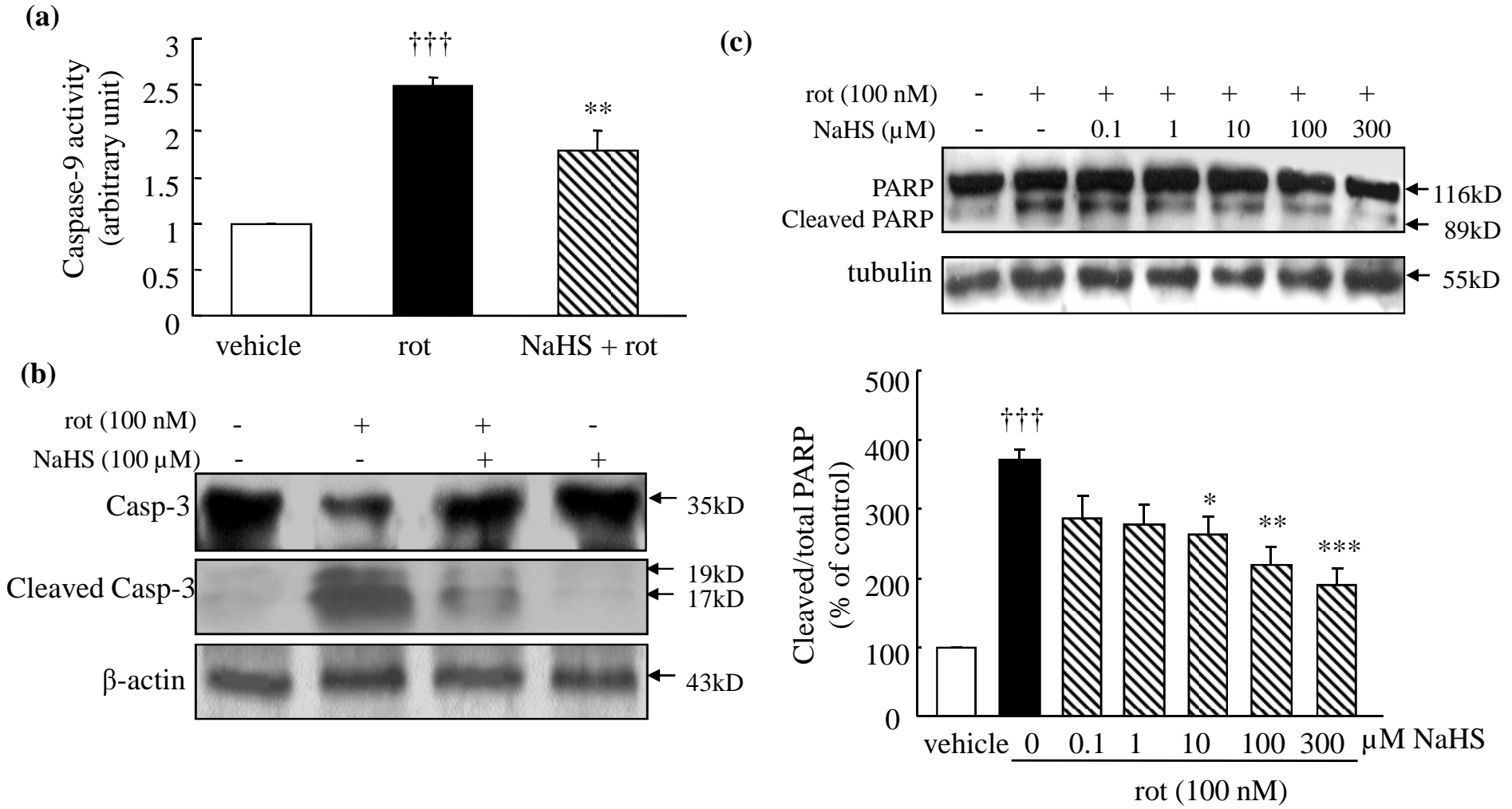




Figure 7

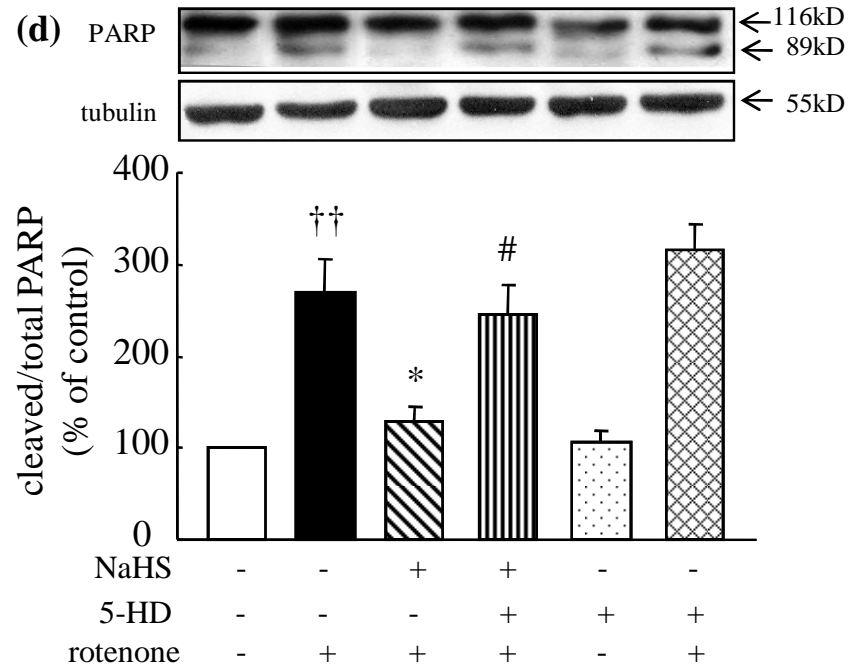
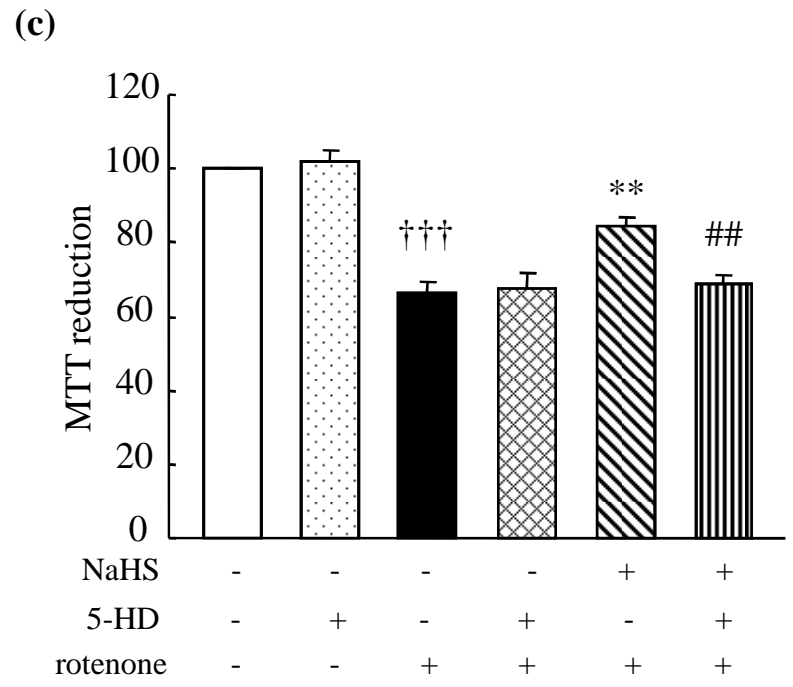
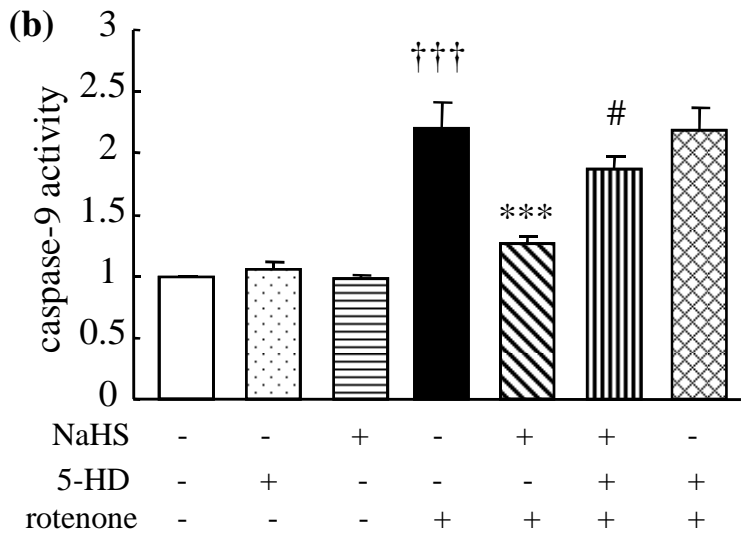
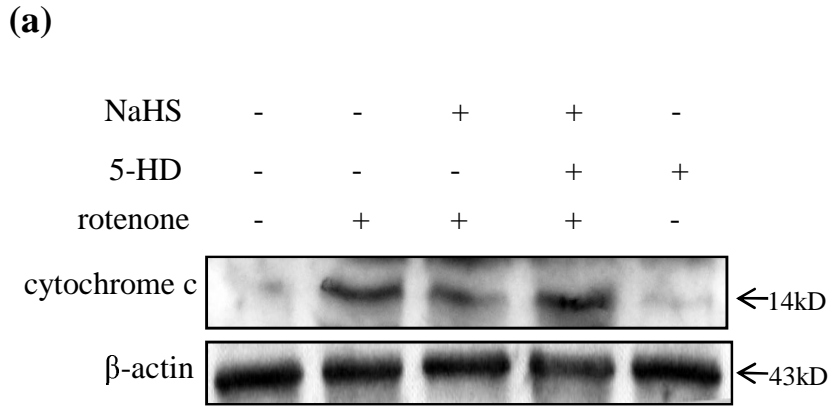


Figure 8

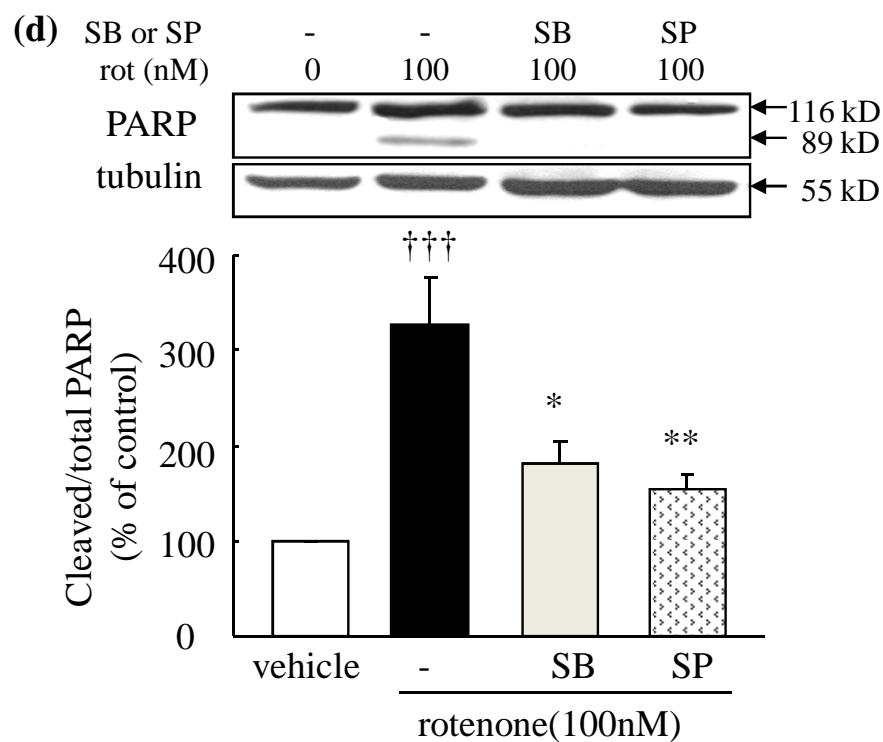
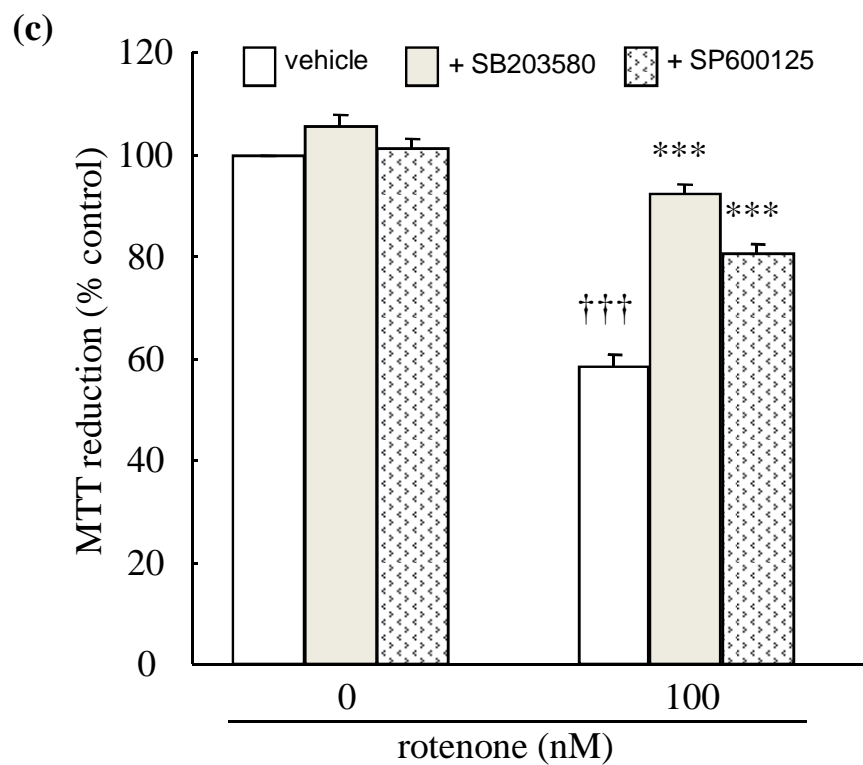
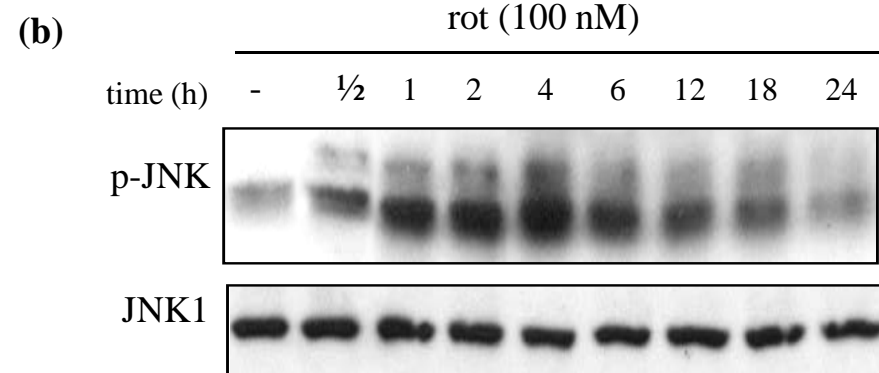
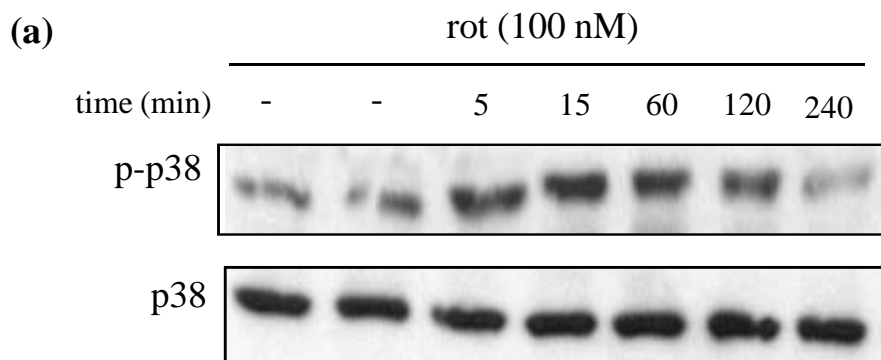


Figure 9

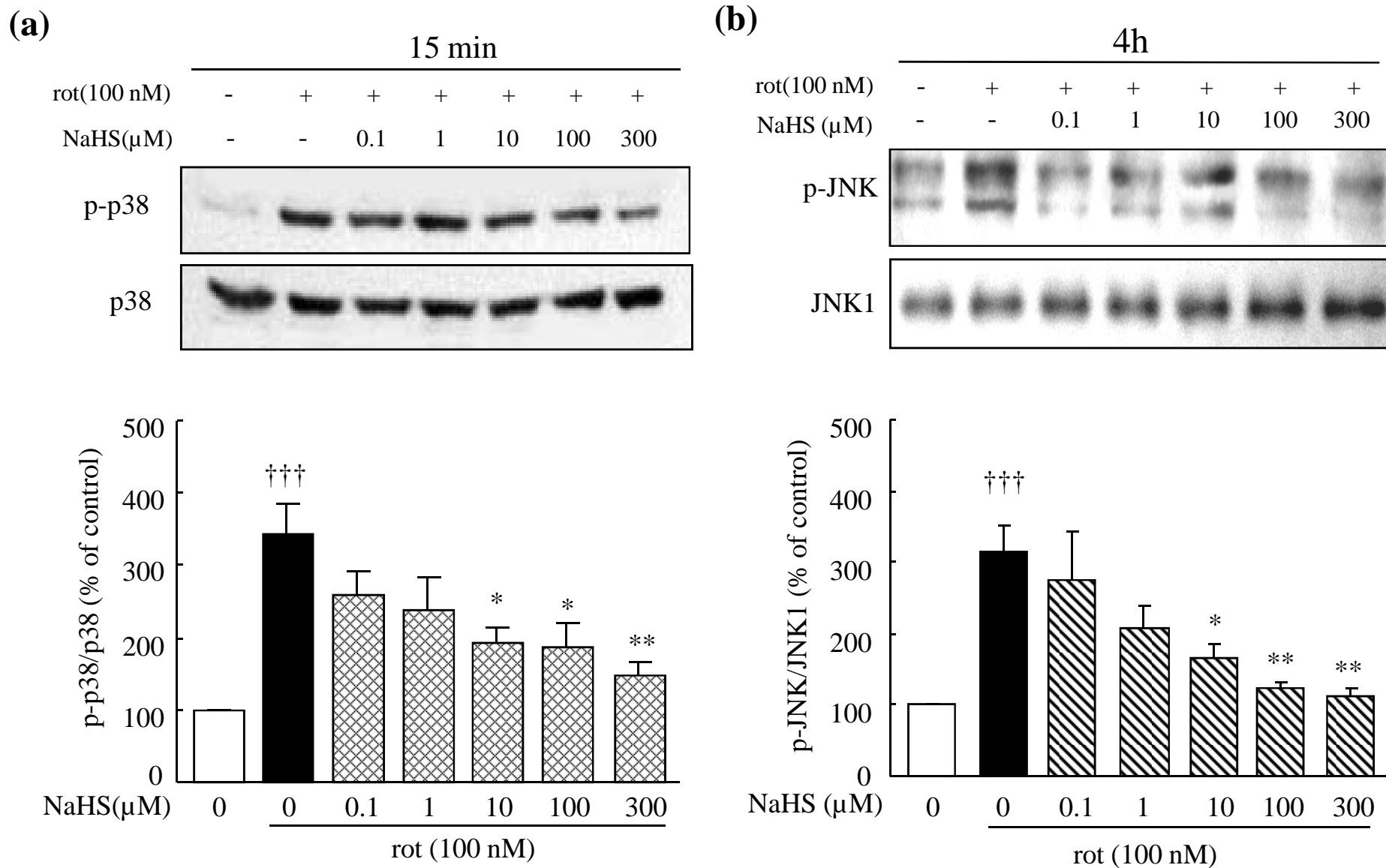


Figure 10

